A Study on the Treatment of Open Boundary in the Two-Dimensional Free-Surface Wave Problems

Yong-Hwan Kim*

(From T.S.N.A.K., Vol. 29, No. 3, 1992)

Abstract

This paper deals with the treatment of the open boundary in two-dimensional free-surface wave problems. Two numerical schemes are investigated for the implementation of the open boundary condition. One is to add the artificial damping term to the dynamic free-surface boundary condition, in which the determination of suitable damping coefficient and the damping zone is the most important. The other is a modified Orlanski's method, which is known to be very useful for the uni-directional waves. Using these two schemes, numerical tests have been conducted for a few typical free-surface wave problems. To obtain the numerical solution of the free-surface boundary value problem, the fundamental source-distribution method is used and the fully nonlinear free-surface boundary conditions are applied. The computed results are presented in comparison with those of others for the proof of practicality of these two schemes.

1. INTRODUCTION

In the numerical computation of free-surface waves in infinite domain, the application of a suitable condition on the truncated boundary is one of the most difficult tasks. The various kinds of numerical treatments of the open boundary problem can be found from the works of Bai[1], Dommermuth & Yue[2], Chan[3], Baker & Orszag[4], Kim[5] and many others and the most wide-spread method among them is to match with the linear solution at the truncated boundary. However, in some cases, it is not so easy to obtain exact linear solution. For example, we need a great effort to compute the Green function of Havelock source. Moreover, this method is not applicable when the large-amplitude wave reaches the truncated boundary and the truncated boundary should be far enough to neglect the nonlinear effects.

In the present study, two methods are introduced for the treatment of open boundary. One adds the artificial damping to the free-surface boundary condition to damp out the motion of free surface. This method has been used by Baker & Orszag[4], and Cointe[6]. Applying the artificial damping over the finite zone, so-called damping zone, on the free-surface adjacent to the truncated boundary, we can eliminate the waves before they reach the boundary of

*Member, DAEWOO Shipbuilding & Heavy Machinery Ltd.

computational domain. The other method is the Orlanski's method which has been used by Chan[3], Yen & Hall[7]. This method is originally suggested by Orlanski[8] to solve the wave problems of compressible fluid. In the present computation, Orlanski's method is modified to solve nonlinear wave problems. The fundamental source-distribution method is applied to solve initial boundary-value problems and the boundary of free surface is obtained adopting semi-Lagrangian time stepping scheme.

2. THE VIBRATION ANALYSIS OF A STRUCTURE IN WATER

It is well-known that the velocity potential defined in the domain of ideal fluid can be obtained by distributing the singularities with the strength to satisfy the boundary conditions. The boundary element method based on this fact has been widely used to solve free-surface wave problems.

Although the numerical damping exists intrinsically in boundary element method, it is not an intended one but resulted purely from the errors in discretization of time and space. The concept of artificial damping is different with that of numerical damping. If one want to damp the motion of free surface compulsorily, the following equation is applicable as the dynamic free-surface boundary condition.

$$\Phi_t + \frac{1}{2}|\nabla\Phi|^2 + g\eta + \mu\Phi = 0 \tag{1}$$

where Φ, g, η, μ are velocity potential, gravitational acceleration, the elevation of free surface, and fictitious damping coefficient respectively. The subscript denotes the differentiation with respect to the subscript parameter. The concept of damping introduced here is different from the real mechanism of viscous damping. This damping term differs as well from the numerical damping of Rankine source method suggested by Dawson[9] in that it is added for the control of wave amplitude. We can also find the damping term, $\mu\Phi$, in the classical wave-resistance problem for the satisfaction of radiation condition. However, the intention of present adoption is not to decide the direction of wave but to eliminate the waves on free surface.

As an example, let's consider the wave-maker problem with finite depth(Fig.1). The velocity potential should satisfy following conditions.

$$\nabla^2\Phi = 0 \quad \text{in the fluid domain} \tag{2}$$

$$\Phi_t + \frac{1}{2}|\nabla\Phi|^2 + g\eta + \mu\Phi = 0 \qquad \text{on } y = \eta \tag{3}$$

$$\eta_t + \Phi_x\eta_x - \Phi_y = 0 \qquad \text{on } y = \eta \tag{4}$$

$$\Phi_y = 0 \qquad \text{on } y = -d \tag{5}$$

$$\Phi_x = A\cos(\omega t) \qquad \text{on } S_M \ \&\ t \geq 0 \tag{6}$$

To apply semi-Lagrangian time stepping technique, two free-surface boundary conditions should be modified as following forms:

$$\frac{D\Phi}{Dt} = \frac{1}{2}|\nabla\Phi|^2 - g\eta - \mu\Phi \tag{7}$$

$$\frac{D\vec{r}}{Dt} = \nabla\Phi \tag{8}$$

or

$$\frac{D\Phi}{Dt}\Big|_{x-fix} = -\frac{1}{2}|\nabla\Phi|^2 - g\eta - \mu\Phi + \Phi_y\frac{D\eta}{Dt} \tag{9}$$

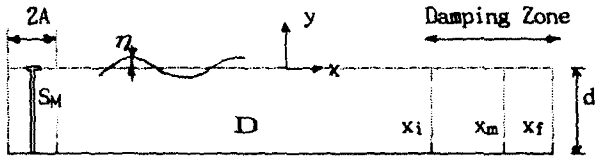

Figure 1: Coordinate system of wave-maker problem

$$\frac{D\eta}{Dt}\Big|_{x-fix} = \Phi_y - \eta_x \Phi_x \tag{10}$$

The free-surface profile can be determined by solving these equations with time- marching.

In the study of Baker[4] and Cointe[6], the artificial damping term was added to the kinematic as well as the dynamic condition. Though such treatment may reduce the elevation more quickly, it is believed that there is no physical reason to add the damping term to the kinematic condition redundantly, since the reduction of free-surface elevation is achieved more naturally as a consequence of dynamical treatment. In the present study, the damping term is included only in the dynamic boundary condition.

A fundamental source-distribution method is used to solve the initial boundary-value problem of equation (2)-(6). Numerical stability is improved using Adams-Bashforth-Moulton's predictor-corrector method for time integration. And short waves are removed using the filtering technique. It is known that the damping effect can be expected in filtering and it is explained in Appendix A.

The value of damping coefficient μ is defined as belows in the present application.

$$\mu = \begin{cases} 0 & \text{if } x < x_i \\ \mu_{max}\sin^2\{\pi(x_m - x)/(x_m - x_i)/2\} & \text{if } x_i \le x < x_m \\ \mu_{max} & \text{if } x_m \le x_f \end{cases} \tag{11}$$

The region of $x_i \le x < x_f$ is called 'damping zone' (Fig.1). The most important parameter is the value of μ_{max}, which should be determined in consideration of tuning with the surface waves. If this value is too small, generated waves will reach the truncated boundary. These waves will reflect and be mixed with the newly-generated waves. If the value of μ_{max} is too high, the waves will be damped very fast. However, in this case, the reflection waves will be generated by the damping zone.

Introducing the basic theory of vibration, we can find the critical value of μ_{max} which can tune to a particular wave(Faltinsen[10]). The critical damping coefficient for the oscillation with the frequency of ω can be expressed as following(see Appendix B).

$$\mu_{cr} = 2\omega \tag{12}$$

The size of damping zone is also important. It can be easily understood that the size is dependent on wave length and the value of damping coefficient. The damping zone should be large enough to damp the fluid motion completely. And careful consideration should be made in the determination of the coordinate of x_m.

Fig.2 shows the computed result of wave-maker problem in the case of $\omega = 4.16$, and this figure shows the effect of artificial damping very well. Figure (a) and (b) are the wave profiles in the cases that the damping zone is from $x/d = 0.0$ to $x/d = 10.0$ and $\mu_{max} = \mu_{cr}, 0.5\mu_{cr}$.

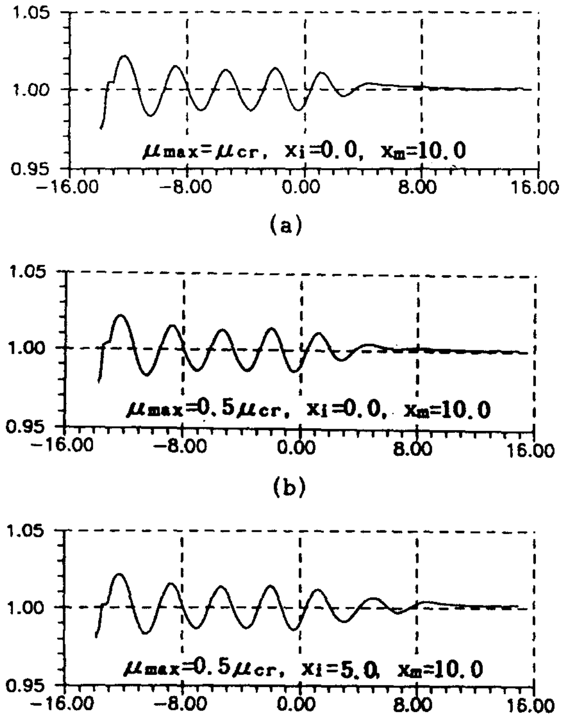

Figure 2: Surface elevations generated by wave maker with various damping zone (μ_{cr} = 8.38, $d = 1.0$)

And figure (c) is for the case that the damping zone is shorter than those of case(a) and (b). The waves generated by wave maker are damped and finally disappear in damping zone. We cannot find any large reflection waves. And it is observed that the wave of case (c) is less damped than those of case (a) and (b) because of short damping zone.

Another computed model is the wave generation by pulsating pressure patch. The pressure on free surface is assumed as

$$p(x,t) = \begin{cases} p_{max}\cos(\pi x/L)\sin(\omega t) & \text{for } -L < x < L \\ 0 & \text{for } -L > x, L < x \end{cases} \tag{13}$$

In the present computation, the right and left boundary is assumed to be rigid walls. No additional condition is adopted in left side but the damping zone is adopted in right side. Fig.3 shows the surface profile at three different time.

It is observed that the reflection waves exist in left side. On the contrast, there is no reflection wave in right side. Fig.4 shows the evolution of free-surface wave with respect to time. At the left side, the contour of reflection wave can be seen. But there is no significant contour of reflection wave in damping zone.

There are a few disadvantages in the application of artificial damping. First of all, computational domain should be large, since computational domain contains the damping zone. Consequently, the domain in consideration must be extended to the damping zone. Another critical problem in the application of this method is the difficulty in determining the value damping coefficient when the wave has many frequency components. According to equa-n (12), the maximum value of damping coefficient depends on only frequency of wave. If nerated wave has the several significant components of different frequencies, it is difficult determine the suitable value of μ_{max}. Therefore, further study is required to solve these roblems for more efficient use of artificial damping.

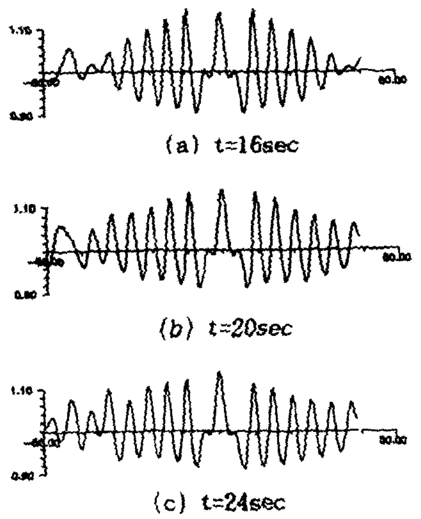

Figure 3: Surface elevation generated by pulsating pressure patch ($\mu_{\max} = \mu_{cr}$, $\sigma = \pi$, $d = 1.0$, $L = 5.0, p_{\max} = 5.0$, Damping zone $= 40 - 50$)

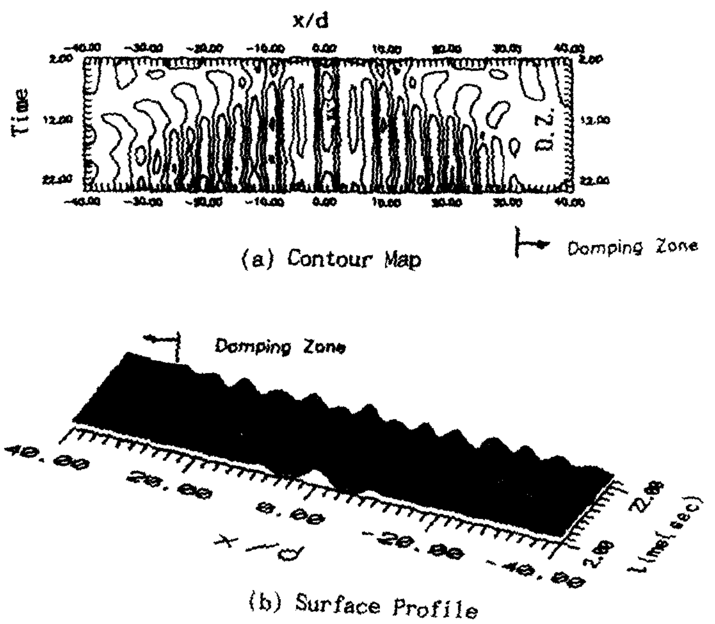

Figure 4: Wave evolution by pulsating pressure patch (Same condition as Fig.3, Damping zone = 30-40)

3. THE APPLICATION OF MODIFIED ORLANSKI'S METHOD

One of the most wide-spread treatment of the radiation condition in the unbounded free-surface wave problem is to apply the Sommerfeld's condition. This method is to adopt the wave equation of hyperbolic type at the matching boundary of inner and outer region. And it is expected for this method to give good result in uni-directional wave problem. After Orlanski[9] used this method for compressible flow, Chan[3], Yen & Hall[7], Wu & Wu[11] and Yang[12] have applied this method for free-surface wave problems. In particular, this method is thought to be valid for highly nonlinear wave problems. This method is based on the assumption that the fluid motion in matching boundary has the characteristics of the wave which is satisfied with Sommerfeld's radiation condition,

$$Q_t + CQ_x = 0 \tag{14}$$

Here Q is any physical parameter that has the characteristics of wave and C is the phase velocity of wave. Q can be velocity potential or free-surface elevation. If the wave has only one component, C will be defined as one value. Otherwise, C will be a local phase velocity which is a function of time and space.

In the present study, phase velocity is computed using the equation suggested by Chan as belows,

$$C = \begin{cases} \Delta x/\Delta t & \text{if } C^* > \Delta x/\Delta t \\ C^* & \text{if } 0 \le C^* \le \Delta x/\Delta t \\ 0 & \text{if } C^* < 0 \end{cases} \tag{15}$$

$$C^* = \frac{\Delta x}{2\Delta t}\frac{Q_{nf-1}{}^{n} + Q_{nf-2}{}^{n-1} - Q_{nf-1}{}^{n-1} - Q_{nf-2}{}^{n-2}}{Q_{nf-2}{}^{n-1} Q_{nf-1}{}^{n-1}} \tag{16}$$

where superscript means the number of time step and subscript $nf - i$ means the $i-$th position from matching boundary. For the evaluation of velocity potential and free-surface elevation at the matching boundary, a finite difference equation such as (16) is generally used in Orlanski's method. The predicted velocity potential and free-surface elevation are adopted as radiation condition. This scheme is based on the concept of extrapolation. However, in the present study, following conditions are used instead of applying finite difference equation.

$$\Phi(t+\Delta t, x_{nf}) \quad = \Phi(t, x_{nf} - C\Delta t)\eta(t+\Delta t, x_{nf}) \quad = \eta(t, x_{nf} - C\Delta t)$$

There are several critical problems in the application of conventional scheme to large-amplitude wave problems, especially in the application of semi-Lagrangian time stepping scheme. For example, when the wave amplitude is very large, the fluid particles near matching boundary can move to the outer region since Lagrangian frame is adopted to trace the motions of fluid particles on free-surface. But such problems can be solved if condition (17) is employed.

Let's consider the solitary wave generated from initial hump as shown in Fig.5. Solitary wave is a representative of shallow water wave and propagates for one direction. Initial elevation is assumed as

$$\eta = 0.5\eta_0(1 + \cos(\pi x/2x_r)) \quad \text{when } t \le 0 \tag{17}$$

At first, the speed of generated solitary wave is observed to validate the present numerical scheme. In this computation, right boundary is assumed to be a rigid wall. Figures 6 and 7 are the computed results. Especially, Figure 7 shows the computational results for the relation between the wave speed and amplitude with those obtained by Wu and Green-Nagdi theory. The present result has more gentle slope. It is presented as a banded region with the deviation since the speed was observed at many points.

Figures from 8 to 11 are the results of the case that equation (17) is applied on matching boundary. Figure 8 shows that the solitary wave passes through the open boundary without any significant reflection. This penetration can be seen in Fig. 9 more clearly. Fig. 10 shows the effect of initial elevation.

Two parameters, velocity potential and elevation, can be used for the computation of phase velocity, and the results may be different for two cases. Fig. 11 shows the comparison of such two results. Fortunately, the difference is not significant.

Another model studied here is the wave generation by pressure patch in uniform current. This problem has been studied by many hydrodynamicists, like Salvensen[13]. Recently, Lee[14] performed numerical computation adopting FEM and he applied the concept of buffer zone for open boundary. Considering the uniform current with velocity U, we can modify free-surface boundary condition as follows:

$$\frac{D\Phi}{Dt}\Big|_{x-fix} = -\frac{1}{2}|\nabla\Phi|^2 - g\eta - U\Phi_x + \Phi_y\frac{D\eta}{Dt} \tag{18}$$

$$\frac{D\eta}{Dt}\Big|_{x-fix} = \Phi_y - \eta_x(\Phi_x + U) \tag{19}$$

To compute the wave slope at $i-$ th position, the following equation is used in present computation.

$$\begin{aligned}\eta_x = \; & (1-\alpha)(-\eta_{i+2} + 8\eta_{i+1} + \eta_{i-2}/(12\Delta x) \\ & \alpha(\eta_{i-2} - 4\eta_{i-1} - 3\eta_i)/(2\Delta x)\end{aligned} \tag{20}$$

where α is a weight factor for one-sided difference. The 3-point filtering suggested by Shapiro is applied at several points near open boundary(Appendix A.). This filtering scheme gives a large numerical damping and it is expected to eliminate short waves reflected at the open boundary. The pressure distribution on free surface is as follows:

$$p(x,t) = \begin{cases} p_{max}\cos^2(\pi x/L) & \text{for } -L < x < L \\ 0 & \text{for } -L > x, L < x \end{cases} \tag{21}$$

Figures 12 and 13 are the computed results for $L/d = 0.525$, $P_{max}/\rho g d = 0.0145$, $U/\sqrt{gd} = 0.572$, and $\alpha = 0.5$. Here, ρ is the density of fluid. Figure 12 shows the propagation of wave to downstream with time-marching. The significant reflection wave is not observed. Figure 13 shows the computed wave elevation in comparison with that of Salvensen, and the wave length of present computational result is shorter than that of Salvensen.

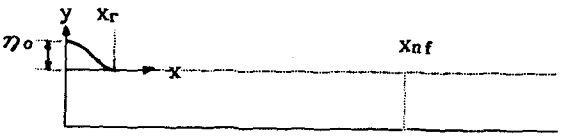

Figure 5: Cordinate system of solitary wave problem

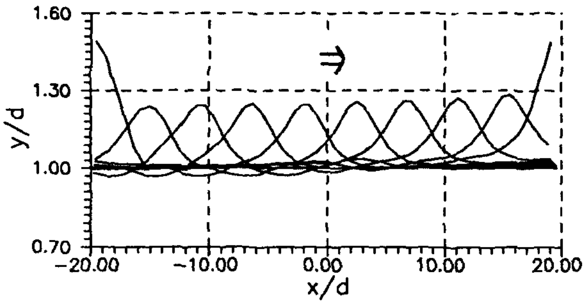

Figure 6: Generation of solitary waves from initial hump, $x_{nf}/d = 40.0$, $a/d = 0.5$, $x_r/d = 5.0$, $\Delta t = 3.92$

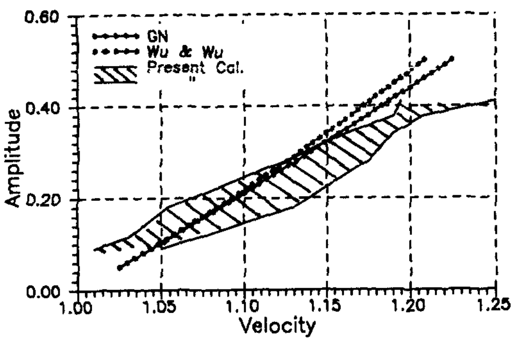

Figure 7: Speed vs. amplitude of solitary waves

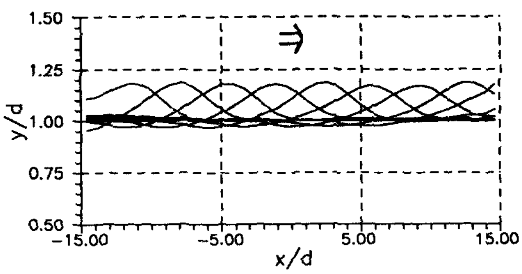

Figure 8: Propagation of solitary wave in open-boundary domain $a/d = 0.4$, $x_r = 5.0$, $\Delta t =$ 3.136

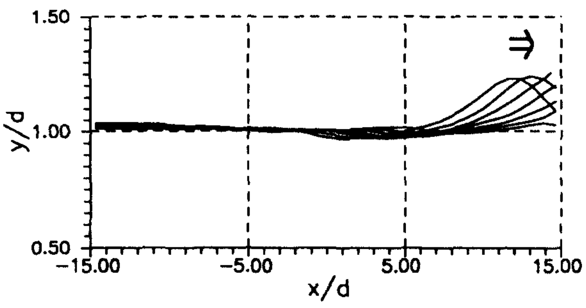

Figure 9: Wave passing-through an open boundary $a/d = 0.5$, $x_r = 5.0$, $\Delta t = 0.44$

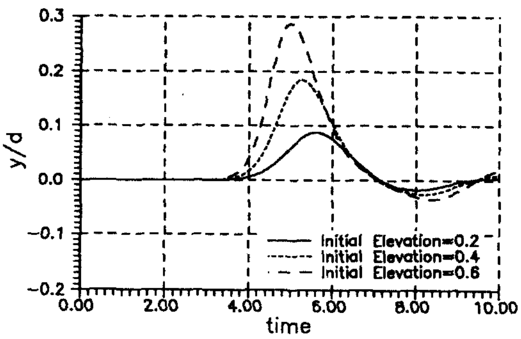

Figure 10: Time variation of elevation at fixed X-coordinate $x_{nf}/d = 40.0$, $a/d = 0.2, 0.4, 0.6$, $x_r = 5.0$

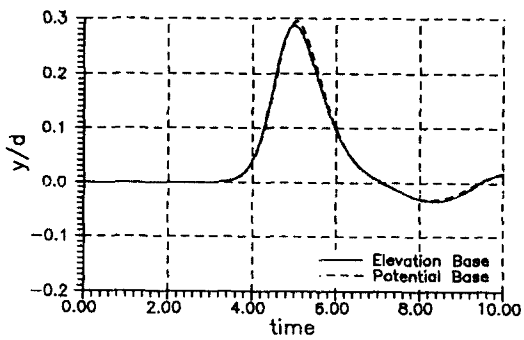

Figure 11: Time variation of elevation at fixed X-coordinate $x_{nf}/d = 40.0$, $a/d = 0.6$, $x_r = 5.0$

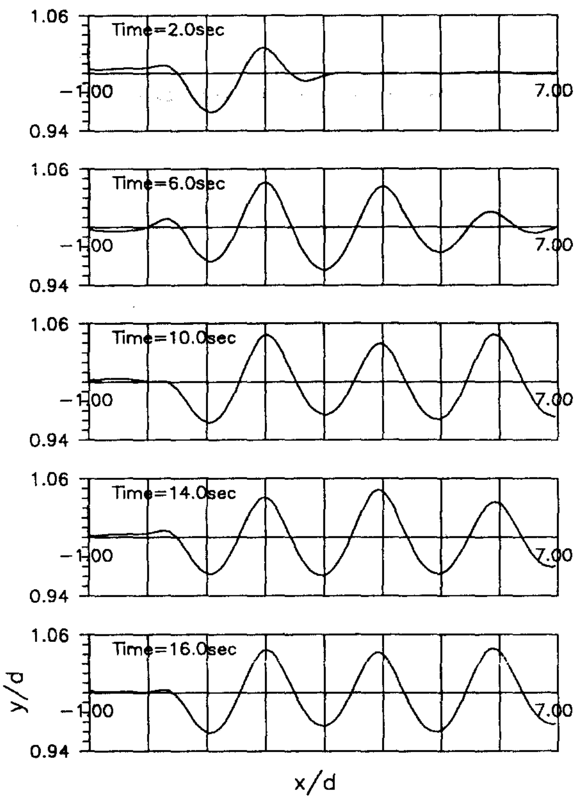

Figure 12: Wave evolution near the pressure patch in uniform stream (matching at $x/d = 9.5$)

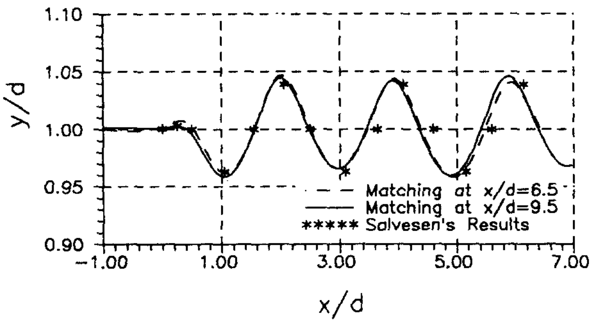

Figure 13: Comparison of wave elevation with Salvesen's result

4. CONCLUSION

In the present study, two numerical techniques for the treatment of open-boundary in the two-dimensional free-surface wave problems are investigated. In the first scheme, the concept of artificial damping is introduced to eliminate the waves before they reach the open boundary. In the second one, the modified Orlanski's method is applied to transmit the waves through the matching boundary without any significant reflection of waves.

The method which eliminates the waves by applying artificial damping is expected to be widely used for various free-surface wave problems. For more pertinent application of artificial damping, careful consideration is required to determine the size of damping zone and the value of damping coefficient and there are a few difficulties to be studied further.

Modified Orlanski's method, proved to transmit waves through the truncated boundary without any significant reflection, is recommendable for uni-directional wave problems. From the numerical tests in the present study, this method seems to work very well for the analysis of nonlinear waves.

References

[1] Bai, K.J. & Yeung, R.W., "Numerical solutions to free-surface flow problems", *Proc. of 10th Sym. on Naval Hydro.*, 1974

[2] Dommermuth D.G. & Yue D.K., "The non-linear three dimensional waves generated by a moving surface disturbance", *Proc. of 17th Sym. on Naval Hydro.*, 1988

[3] Chan, Robert, K.C., "Finite difference simulation of the planar motion of a ship", *Proc. of 2nd Int. Con. on Numerical Shiphydro.*, 1977

[4] Baker, G.R., Meiron, D.I. & Orszag, S.A., "Applications of a generalized vortex method to nonlinear free-surface flows", *Proc. of 3rd Int. Con. on Numerical Shiphydro.*, 1981

[5] Kim, J.W., "A Numerical Method for Nonlinear Wave-Making Phenomena", Ph.D. Thesis, Seoul National University, 1991

[6] Cointe, R., "Nonlinear simulation of transient free surface flows", *Proc. of 5th Int. Con. on Numerical Shiphydro.*, 1989

[7] Yen, S.M. & Hall, D.R., "Implementation of open boundary conditions for nonlinear free-surface wave problems", *Proc. of 3rd Int. Con. on Numerical Shiphydro.*, 1981

[8] Orlanski, L., "A simple boundary condition for unbounded hyperbolic flows", *Jour. of Computational Physics*, Vol. 21, 1976

[9] Dawson, C.W., "A practical computer method for solving ship-wave problems", *Proc. of 2nd Int. Con. on Numerical Shiphydro.*, 1977

[10] Faltinsen, O.M., "Numerical nonlinear method of sloshing in tanks with two dimensional flow", *Jour. of Ship Research*, Vol. 22, No.3, 1978

[11] Wu, D.M. & Wu, T.Y., "Three dimensional nonlinear long waves due to moving surface pressure", *Proc. of 14th Sym. on Naval Hydro.*, 1982

[12] Yang, C., Liu, Y.Z. & Takagi, N., "Time domain calculation of the nonlinear hydrodynamics of wave-body interaction", *Proc. of 5th Int. Con. on Numerical Shiphydro.*, 1989

[13] Von Kerczek, C.H.. & Salvesen, N., "Numerical solutions of the two-dimensional nonlinear wave problems", *Proc. of of 10th Sym. on Naval Hydro.*, 1974

[14] Lee, H.S,, "A Numerical Analysis of Two-Dimensional Free-Surface Flow Problem", M.S. Thesis, Seoul National University, 1990

[15] Longuet-Higgins, M.S. & Cokelet, E.D., "The deformation of steep surface waves on water I", *Proc. of Royal Soc.*, Vol. 350, 1976

[16] Shapiro, R., "Linear filtering", Mathematics of Computation, Vol. 29, No.132, 1975

[17] Kim, Y.H. & Park,Y.J., "Analysis of Sloshing Problem by Numerical Method", *Tran. of SNAK*, Vol. 29,. No.3, 1992

Appendix A: The Filtering of Free-Surface Waves

In the numerical computation of free-surface wave problem, the unexpected short wave is generated by numerical error. Numerical stability becomes bad when this short wave becomes significant, and numerical computation cannot be continued at last. The most famous technique to remove this short wave is the smoothing used by Longuet-Higgins & Cokelet[15]. It can be said that their technique is based on the concept of filtering, and the basic filtering technique for free-surface wave can be found at the work of Shapiro[16]. Let's consider a simple filtering equation suggested by Shapiro,

$$\eta^f{}_i = \frac{1}{4}(\eta_{i-1} + 2\eta_i + \eta_{i+1}) \tag{A.1}$$

where $\eta^f{}_i$ is a filtered elevation at x_i considering the elevations of adjacent two points located at $x_i - \Delta x$ and $x_i + \Delta x$. To examine the difference between $\eta^f{}_i$ and η_i , it is assumed that

$$\eta_i = \sum A_n \cos n(x_i - \phi_i) \tag{A.2}$$

Here, A_n is the amplitude of the wave with wave number n. Then the amplitude ratio is

$$R = \left|\frac{A_n{}^f}{A_n}\right| = \frac{1}{2}(\cos n\Delta x + 1) \tag{A.3}$$

If this filtering equation is applied for the wave with the length of $2\Delta x$, we can observe that R is 0 since $n = \pi/\Delta x$. It means that the wave with the length of $2\Delta x$ will disappear after applying this filtering equation. The representative equations and the amplitude ratios of free-surface wave filtering are summarized with the amplitude operators as follows:

(i) Five-point filtering : Method 1

$$\eta^f{}_i = \frac{1}{16}(-\eta_{i-2} + 4\eta_{i-1} + 10\eta_i + 4\eta_{i+1} - \eta_{i+2})$$
$$R = 1 - \sin^4(\pi\Delta x/\lambda)$$

(ii) Five-point filtering : Method 2

$$\eta^f{}_i = \frac{1}{32}(-\eta_{i-3} + 9\eta_{i-1} + 16\eta_i + 9\eta_{i+1} - \eta_{i+3})$$
$$R = \frac{1}{16}(-\cos(6\pi\Delta x/\lambda) + 9\cos(2\pi\Delta x/\lambda) + 8)$$

(iii) Seven-point filtering

$$\eta^f{}_i = \frac{1}{64}(\eta_{i-3} - 6\eta_{i-2} + 15\eta_{i-1} + 44\eta_i + 15\eta_{i=1} - 6\eta_{i=2} + \eta_{i=3})$$
$$R = 1 - \sin^6(\pi\Delta x/\lambda)$$

(iv) Nine-point filtering

$$\eta^f{}_i = \frac{1}{256}(-\eta_{i-4} - 8\eta_{i-3} - 28\eta_{i-2} + 56\eta_{i-1} + 186\eta_i + 56\eta_{i+1} - 28\eta_{i+2} + 8\eta_{i+3} - \eta_{i+4})$$
$$R = 1 - \sin^8(\pi\Delta x/\lambda)$$

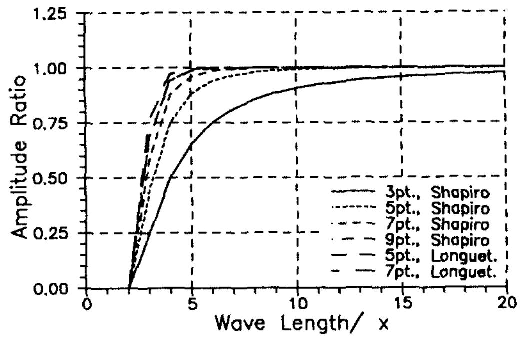

Figure 14: Amplitude ratio vs. wave length

In most of unsteady wave problems, the numerically-generated short wave can be removed using this filtering scheme. However, it must be noticed that there is numerical damping in filtering scheme. When excessive or unsuitable application is made, wrong results may be given. Figure 15 shows the influence of the time-segment interval that filtering is applied. This figure is the the time-history of surface elevation at fixed point in two-dimensional rectangular tank after sudden impact. It can be seen that 3 point filtering gives over-damping. In unsteady problem, the filtering should be repeated as time-step increases, and this repetition can induce the phase distortion.

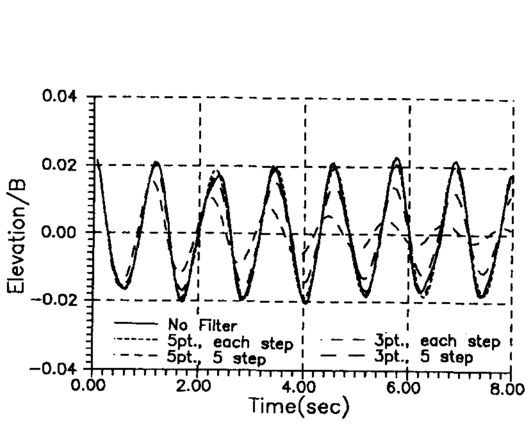

Figure 15: Effect of filtering(free oscillation test) $h/B = 0.5$, linear initial elevation, maximumheight$/B = 0.1$

Appendix B: Linear Free-Surface Waves & Artificial Damping

The effects of artificial damping on linear free-surface wave can be easily examined from the basic theory of vibration. Let's consider following linear free-surface wave problem including the artificial damping term $\mu\Phi_t$.

$$\nabla^2\Phi = 0 \quad \text{in fluid domain} \tag{B.1}$$

$$\Phi_{tt} + \mu\Phi_t + g\Phi_y = 0 \quad \text{on free surface } (y = 0) \tag{B.2}$$

$$\Phi_y = 0 \quad \text{on bottom boundary } (y = -d) \tag{B.3}$$

Applying the separation of variables, we can assume the form of velocity potential as follows:

$$\Phi = X(x)Y(y)T(t) \tag{B.4}$$

The time-dependent term, $T(t)$, should satisfy following partial differential equation.

$$T_{tt} + \mu T_t + \sigma^2 T = 0 \tag{B.5}$$

Here,

$$\sigma^2 = gk\tanh(kd) \tag{B.6}$$

and k, $sigma$ are wave number and wave frequency. Therefore, $T(t)$ can be expressed as follows:

$$T(t) = C_1 exp(s_1 t) + C_2 exp(s_2 t) \tag{B.7}$$

where

$$s_{1,2} = \frac{1}{2}(-\mu \pm \sqrt{\mu^2 - 4\sigma^2}) \tag{B.8}$$

s_1, s_2 will play an important roll to determine the damping ratio with respect to time. According to equation (B.8), the critical damping coefficient, μ_c, for the wave of frequency *sigma* is

$$\mu_c = 2\sigma \tag{B.9}$$

If the damping coefficient is less than this value, the characteristics of wave will sustain while the amplitude would be reduced. On the contrary, if the damping coefficient is greater than μ_c, the characteristics of wave would disappear immediately. For example, let's consider the fluid motion trapped in two-dimensional rectangular tank. If the breadth of tank is B and the filling-depth is d, the wave frequency of fundamental natural mode is

$$\sigma = \sqrt{g\pi \tanh(\pi d/B)/B} \tag{B.10}$$

Figure 16 shows the time-history of free-surface elevation observed at fixed x-coordinate. In this case, it is assumed that there is an initial elevation and the fluid motion is in free oscillation. Besides, the exact nonlinear free-surface condition is applied. In this figure, we can see clearly the effects of the artificial damping. Although a fully nonlinear condition is adopted, the computed results exactly coincide with the theory explained above.

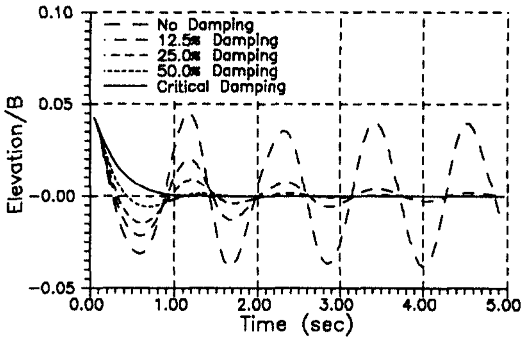

Figure 16: Free oscillation test in rectangular tank $d/B = 0.5$, linear initial elevation, $\text{maximumheight}/B = 0.2$

Figure 17 shows the computed results in the case that the tank motion is under excitation. The detailed method of this problem is explained in the paper of Kim[17]. This result shows that the fluid motion is dependent on the value of artificial damping. From this figure, we can see that the adoption of suitable artificial damping can give good result. It means that the real mechanism to damp the fluid motion can be simulated using the appropriate use of artificial damping.

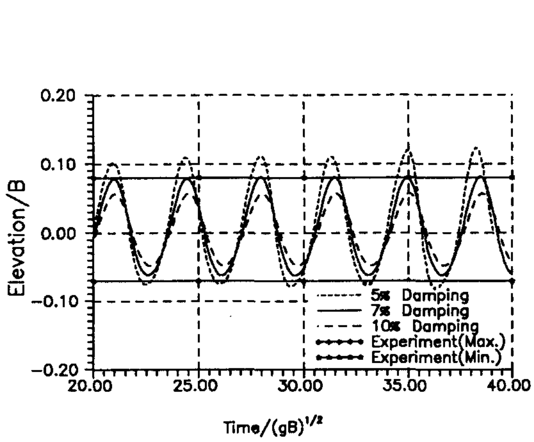

Figure 17: Free-surface elevation in rectangular tank sway motion, 50% filling, motion amlitude/breadth=0.0083, exciting frequency/σ_n = 1.018